Fermionic Suppression of Dipolar Relaxation

Nathaniel Q. Burdick,[1,3] Kristian Baumann,[1,3] Yijun Tang,[2,3] Mingwu Lu,[1,3] and Benjamin L. Lev[1,2,3]
[1]*Department of Applied Physics, Stanford University, Stanford, California 94305, USA*
[2]*Department of Physics, Stanford University, Stanford, California 94305, USA*
[3]*E. L. Ginzton Laboratory, Stanford University, Stanford, California 94305, USA*
(Received 14 July 2014; revised manuscript received 24 August 2014; published 14 January 2015)

We observe the suppression of inelastic dipolar scattering in ultracold Fermi gases of the highly magnetic atom dysprosium: the more energy that is released, the less frequently these exothermic reactions take place, and only quantum spin statistics can explain this counterintuitive effect. Inelastic dipolar scattering in nonzero magnetic fields leads to heating or to loss of the trapped population, both detrimental to experiments intended to study quantum many-body physics with strongly dipolar gases. Fermi statistics, however, is predicted to lead to a kinematic suppression of these harmful reactions. Indeed, we observe a 120-fold suppression of dipolar relaxation in fermionic versus bosonic Dy, as expected from theory describing universal inelastic dipolar scattering, though never before experimentally confirmed. Similarly, low inelastic cross sections are observed in spin mixtures, also with striking correspondence to predictions. The suppression of relaxation opens the possibility of employing fermionic dipolar species in studies of quantum many-body physics involving, e.g., synthetic gauge fields and pairing.

DOI: 10.1103/PhysRevLett.114.023201 PACS numbers: 34.50.-s, 03.65.Nk, 67.85.-d

Spin statistics play a prominent role in determining the character and rate of elastic collisions among ultracold atoms or molecules [1–3], often leading to the enhancement or suppression of thermalization. For example, elastic collisions mediated by short-range interactions between spin-polarized fermions are suppressed at low velocity. The reason lies in the requirement that the total two-particle state—the tensor product of spin and orbital—must be antisymmetric both before and after a collision [4]. Because the orbital wave function must be of odd parity for spin-polarized fermions, collisions between two such atoms are inhibited by the p-wave centrifugal energy barrier [5]. For van der Waals interactions, this leads to a kinematic suppression of the elastic cross section as $k_i \to 0$, where the wave vector k_i is proportional to the relative incoming momentum. The fermionic suppression of thermalizing elastic collisions has an important, well-known consequence: inefficient evaporative cooling near quantum degeneracy [6].

This unfavorable scaling is modified in the case of 3D dipolar interactions. The long-range, r^{-3} nature of the dipolar interaction leads to an elastic cross section independent of k_i and proportional to the fourth power of the magnetic dipole moment μ regardless of quantum statistics in the limit $k_i \to 0$ [7–9] [10]. This manifestation of "universal" elastic dipolar scattering implies that sufficiently strong dipolar interactions allow spin-polarized fermions to evaporatively cool even at energies comparable to and below the Fermi temperature T_F [11]. Indeed, recent experiments employing the highly dipolar fermionic gases KRb [3], Dy [13], and Er [14], have observed efficient evaporative cooling at T_F and below, providing a route to preparing quantum degenerate dipolar Fermi gases without the use of sympathetic cooling [15].

But while large dipoles promote useful elastic collisions, they also enhance inelastic dipolar collisions among atoms in metastable Zeeman substates. Rapid heating or population loss are a result of the ensuing spin relaxation [16] and are detrimental to experiments exploring quantum many-body physics or atom-chip magnetometry with highly dipolar gases in metastable spin states [18–24]. Inelastic dipolar collisions among highly magnetic atoms in magnetostatic traps were considered in the context of bosonic Cr gases at fifty to hundreds of μK [7] and at a few hundred nK [9] and Dy gases at hundreds of mK [25] and at a few hundred μK [26]. The authors of Ref. [7] derived an expression for inelastic dipolar scattering using the first-order Born approximation and observed rapid collisional loss in a single isotope of bosonic Cr. See also Ref. [1]. While the loss rate proved similar to that expected from theory, the theory's general applicability was unexplored. Reference [9] discussed the role of Fermi statistics in dipolar relaxation, noting that—despite the long-range nature of elastic dipolar scattering—dipolar relaxation is a short-ranged scattering process and should exhibit kinematic suppression similar to elastic scattering via the van der Waals interaction. Though predicted, this suppression was not experimentally investigated.

By comparing dipolar relaxation rates in both ultracold bosonic and fermionic dysprosium, we find that spin relaxation is enhanced among bosons while suppressed among fermions. With regard to the fermions, we find that the more energy released, the less frequently these exothermic reactions take place, and only quantum spin

statistics can explain this counterintuitive effect. The strikingly close correspondence of our spin relaxation data to theoretical predictions—with no free parameters—represents a clear demonstration of the role quantum statistics plays in universal inelastic dipolar scattering: i.e., these results should apply to any species whose collisions are dominated by dipolar scattering.

Following Refs. [7,9], we now describe two-particle dipolar scattering within the first-order Born approximation, and in doing so quantify the role quantum statistics play in suppressing or enhancing dipolar relaxation. Dipolar scattering changes the orbital momentum of the collision partners by $\Delta l = 0, \pm 2$ and the spin projection of one or both of the atoms by $\Delta m_F = 0, \pm 1$ [1,7]. The total angular momentum projection remains conserved $\Delta m_F + \Delta m_l = 0$, where m_l is the orbital projection.

The dipolar relaxation cross section σ_{DR} connects theoretical predictions to the experimentally measured collisional loss rate β_{DR} via $\beta_{\mathrm{DR}} \propto \langle(\sigma_1 + \sigma_2)v_{\mathrm{rel}}\rangle_{\mathrm{thermal}}$, where a thermal average must be taken, σ_1 (σ_2) is the single (double) spin-flip cross section, and v_{rel} is the relative velocity; see Supplemental Material for details [27]. The following expressions list the cross sections for the elastic (σ_0) and σ_1 processes for a maximally stretched and weak-field-seeking initial two-body spin state $|F, m_F = +F; F, m_F = +F\rangle$ [7,9]:

$$\sigma_0 = \frac{16\pi}{45} F^4 \left(\frac{\mu_0 (g_F \mu_B)^2 m}{4\pi\hbar^2}\right)^2 [1 + \epsilon h(1)], \quad (1)$$

$$\sigma_1 = \frac{8\pi}{15} F^3 \left(\frac{\mu_0 (g_F \mu_B)^2 m}{4\pi\hbar^2}\right)^2 [1 + \epsilon h(k_f/k_i)] \frac{k_f}{k_i}. \quad (2)$$

While the full theory is used in data analysis, we neglect σ_2 in this initial discussion since $\sigma_2/\sigma_1 = F^{-1} \ll 1$ in large-spin atoms polarized in large $|m_F|$ states [27]. This limit is satisfied for bosonic ^{162}Dy ($F = 8$) and fermionic ^{161}Dy ($F = 21/2$); F is the total angular momentum [30].

The kinematic factors in σ_1 are a function of the ratio of output to input relative momenta: by conservation of energy $k_f/k_i = \sqrt{1 + (m\Delta E/\hbar^2 k_i^2)}$, where $\Delta E = g_F \mu_B B$ is the Zeeman energy in a magnetic field B, $k_i = \mu v_{\mathrm{rel}}/\hbar$, $\mu = m/2$ is the reduced mass, and g_F is the g factor [33]. The ratio $h(x = k_f/k_i)$ of the exchange to the direct terms in the cross section monotonically increases from $h(1) = -1/2$ to $h(x \to \infty) = 1 - 4/x^2$; see Refs. [7,27]. The ratio x is varied between 2–14 in this work.

Quantum statistics of the colliding particles are reflected in the value of ϵ: ± 1 for same-species bosons and fermions, respectively, whose spin states are identical either in the incoming or outgoing channel [1], as in Figs. 1(a)–1(e); and 0 for distinguishable particles, such as mixed species or, as in Fig. 1(f), same-species bosons or fermions in mixed spin states both in the incoming and outgoing channels. In the $x \gg 1$ limit—high B, low T—the inelastic cross section

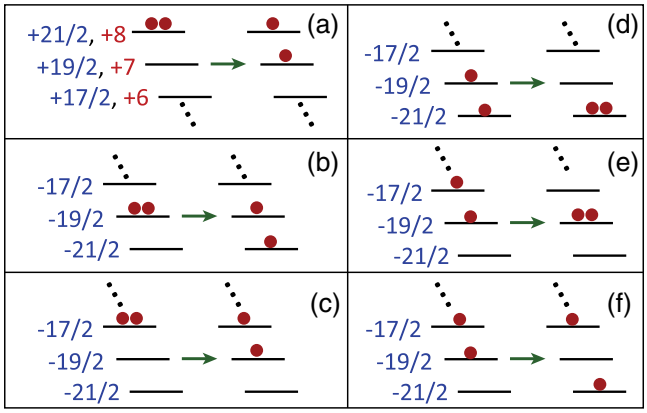

FIG. 1 (color online). (a)–(c) Single-spin-flip dipolar relaxation of spin-polarized states into spin mixtures. Arrow points from the incoming to the outgoing spin population. (d) and (e) Single-spin-flip dipolar relaxation of spin mixtures into spin-polarized states. (f) Single-spin-flip dipolar relaxation of a spin mixture into a different spin mixture.

(collisional loss rate) vanishes as $4\sqrt{T/B}$ ($4T/\sqrt{B}$) for $\epsilon = -1$, while it increases as $2\sqrt{B/T}$ ($2\sqrt{B}$) for $\epsilon = +1$ and $\sqrt{B/T}$ ($\sqrt{B}$) for $\epsilon = 0$. The relative suppression ratio in this limit becomes $\sigma_1^{\mathrm{fermions}}/\sigma_1^{\mathrm{bosons}} = \beta_{\mathrm{DR}}^{\mathrm{fermions}}/\beta_{\mathrm{DR}}^{\mathrm{bosons}} \propto 2T/B$.

Ultracold gases of bosonic ^{162}Dy and fermionic ^{161}Dy are prepared by laser cooling in two magneto-optical-trap stages and by forced evaporative cooling in a 1064-nm crossed optical dipole trap, as explained in previous publications [13,34,35]; see also Ref. [27]. The temperatures of the boson and fermion gases, ~400 nK, are chosen to be slightly above quantum degeneracy to eliminate correlation effects [9]: $T/T_c = 1.5(1)$ [density $3(1) \times 10^{13}$ cm^{-3}] and $T/T_F = 1.4(1)$ [$7(2) \times 10^{12}$ cm^{-3}] [36]. Adiabatic rapid passage while in the optical dipole trap polarizes the atomic cloud in its absolute internal ground state. Cotrapping ^{162}Dy with ^{161}Dy is used to enhance fermionic evaporation efficiency, after which the bosons are removed from the trap by a resonant pushing beam with no adverse effect on the fermions. The atoms are then prepared in the desired Zeeman substate(s) by driving rf transitions, as detailed in Ref. [27]. Stern-Gerlach measurements are used to verify the final state purity.

The atomic cloud is trapped for varying lengths of time in order to measure population decay. Decay curves are fit to a numerically integrated rate equation that includes collision terms for both one-body loss due to background gas γ and two-body loss β_{DR}:

$$\frac{dN}{dt} = -\gamma N - \beta_{\mathrm{DR}} \bar{V}^{-1} N^2, \quad (3)$$

where $\bar{V} = \sqrt{8}(2\pi)^{3/2}\sigma_x\sigma_y\sigma_z$ is the mean collisional volume for a harmonically trapped thermal cloud with

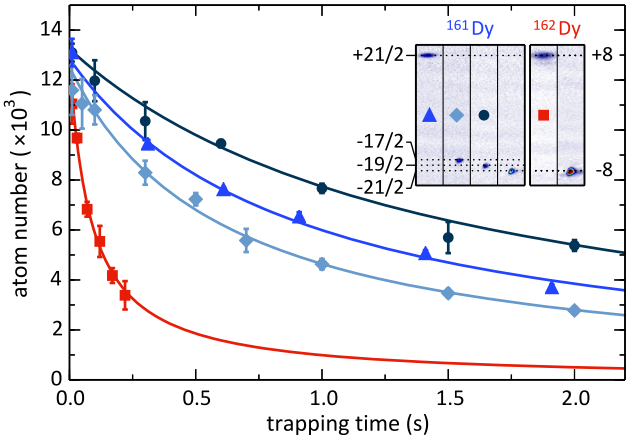

FIG. 2 (color online). Population decay of fermionic ^{161}Dy at $B = 0.410(5)$ G, $T = 390(30)$ nK, and $\bar{n}_0 = 7(2) \times 10^{12}$ cm^{-3} for $m_F = +21/2$ (triangles), $-19/2$ (circles), and $-17/2$ (diamonds) as well as bosonic ^{162}Dy at $B = 0.100(5)$ G, $T = 450(30)$ nK, and $\bar{n}_0 = 3(1) \times 10^{13}$ cm^{-3} for $m_F = +8$ (squares). The solid curves are fits to the data using Eq. (3) [36]. (Inset) Stern-Gerlach images of initial states.

Gaussian widths σ_i [27]. The decay rate is characterized by the lifetime $\tau_{\mathrm{DR}} = (\beta_{\mathrm{DR}}\bar{n}_0)^{-1}$, where $\bar{n}_0 = N_0/\bar{V}$ is the initial mean collisional density.

Typical decay curves for four different spin-polarized ensembles are shown in Fig. 2. The fermions are prepared in either the $m_F = +21/2$, $-19/2$, or $-17/2$ state, as in Figs. 1(a)–1(c), respectively, and the bosons are prepared in the $m_F = +8$ state as in Fig. 1(a). The inset of Fig. 2 contains Stern-Gerlach-separated images of these states as well as the absolute ground states $m_F = -21/2$ and $m_F = -8$. Decay of these states, which cannot undergo dipolar relaxation at this B field and temperature, are not presented due to their much slower decay, limited only by $1/\gamma = 21(1)$ s. Table I lists the experimental decay rates β_{DR} for the $m_F = -19/2$ and $-17/2$ cases, along with the corresponding theoretical predictions. Decays are well described by Eq. (3), as verified by χ^2 analysis [27].

We expect from the form of Eq. (2) that the bosonic lifetime τ_{DR} should decrease as the magnetic field increases, while the fermionic lifetime should increase. Both trends are observed, as shown in Figs. 3(a) and 3(b). While bosonic ^{162}Dy decays rapidly, the fermionic gases at 1 G live for approximately 1 s at this density.

Feshbach resonances can obscure the manifestation of Eq. (2) by increasing losses due to three-body inelastic collisions. Dysprosium has a high density of Feshbach resonances, even at low field [35], and atom loss spectra for the different m_F states were measured prior to investigating the magnetic field dependence of dipolar relaxation. Magnetic fields were selected to avoid increased loss due to sharp Feshbach resonance features in the data of Figs. 2–4. Feshbach spectra for the $m_F = +8$ bosons and $m_F = +21/2$ fermions are shown in Figs. 3(c) and 3(d), respectively; see Ref. [27] for additional spectra.

TABLE I. Collisional loss rates in units of $[\times 10^{-13}$ cm^{-3} s$^{-1}]$.

	$\beta_{\mathrm{DR}}^{-17/2;-17/2}$	$\beta_{\mathrm{DR}}^{-19/2;-19/2}$	$\beta_{\mathrm{DR}}^{-17/2;-19/2}$	$\beta_{\mathrm{DR}}^{-19/2;-21/2}$
Expt.	10(2)	4.1(7)	60(30)	3(1)
Theor.	6.3(3)	4.1(1)	37(1)	4.2(5)

Figure 3(e) presents the β_{DR}'s of the data in Figs. 3(a) and 3(b). Data are in remarkable agreement with the theoretical curves, though the discrepancy of the fermion β_{DR}'s at fields below ~0.2 G warrants further investigation. The errors in β_{DR}'s are dominated by uncertainties in the temperatures and trap frequencies, see Ref. [27].

While the relative suppression is evident in the form of Eq. (2), we may gain a more intuitive understanding of this relative suppression from an analysis of symmetrization, selection rules, and kinematics. Let us first consider the spin relaxation channel depicted in Fig. 1(a) in which spin-polarized fermions or bosons decay from the maximally stretched state $m_F = +F$. This case corresponds to the data in Figs. 3(a) and 3(b), respectively, and to the sets of triangle and square data in Fig. 2. The collisional reaction among fermions may be written

$$|F, m_F; F, m_F\rangle \otimes |p, m_l\rangle \rightarrow |F, m_F - 1; F, m_F\rangle_{\mathcal{S}} \otimes |p, m_l + 1\rangle, \quad (4)$$

where $\mathcal{S}$ denotes the symmetric superposition. While this inelastic collision is allowed by dipolar-interaction selection rules and by symmetrization, the reaction is kinematically suppressed, as we now discuss.

The authors of Ref. [9] explain why kinematic suppression applies to sufficiently exothermic dipolar relaxation in identical fermions but does not apply to elastic dipolar scattering. The elastic dipolar cross section is a manifestation of the long-range nature of the dipolar interaction: all partial waves contribute, even as the collision energy approaches zero. This may be seen by noting that the integral employed to derive the elastic cross section in Eq. (1)—i.e., the integral of the input wave function with $1/r^3$ times the output wave function—involves wave functions spatially oscillating at the same frequency. By contrast, the overlap integral used to derive the inelastic cross section, Eq. (2), involves spatially mismatched wave functions. The outgoing wave function oscillates with a frequency that becomes larger than the incoming wave function's as the collision becomes more exothermic. The contribution to the integral at large relative distance diminishes as the mismatch increases between these wave functions. Fewer higher-order (longer-ranged) partial waves contribute until only that of the lowest s-wave incoming wave function remains: the inelastic dipolar interaction becomes effectively short ranged. We now see why exothermic inelastic dipolar collisions among

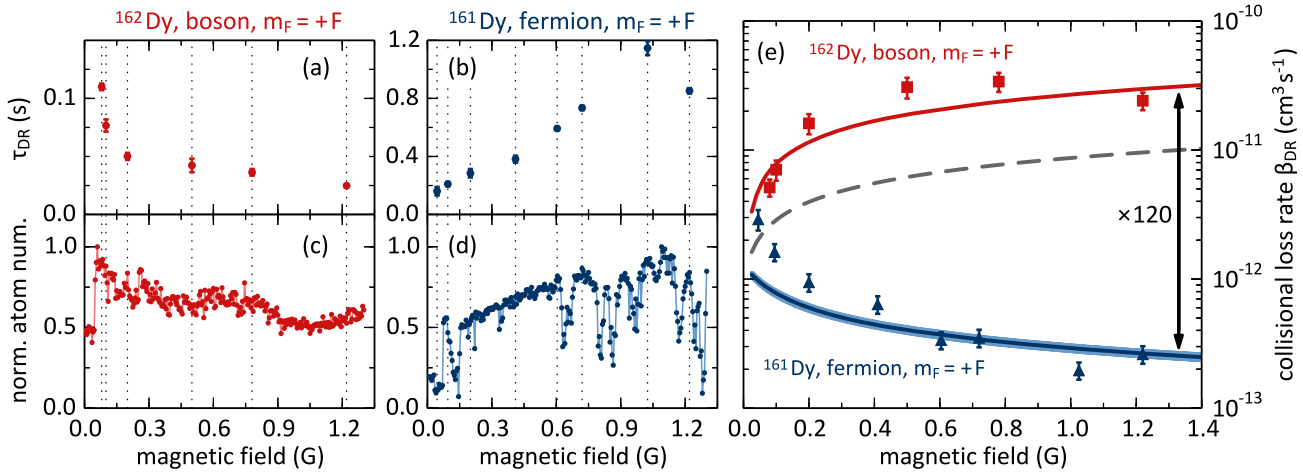

FIG. 3 (color online). Dipolar relaxation as depicted in Fig. 1(a) for bosonic ^{162}Dy ($m_F = +8$) and fermionic ^{161}Dy ($m_F = +21/2$). (a)–(b) Two-body-loss lifetimes versus magnetic field. (c)–(d) Atom loss spectra presented as normalized atom number. Locations of Feshbach resonances appear as dips in the atom loss. (e) Two-body collisional loss rates for ^{162}Dy (squares) and ^{161}Dy (triangles) at the same fields as in (a)–(d). See Fig. 2 caption and Ref. [27] for initial densities and temperatures. Curves are collisional loss rates calculated using the expressions for σ_1 and σ_2 in Eq. (2) and in Ref. [27], respectively, and correspond to ^{162}Dy (top), ^{161}Dy (bottom) and distinguishable particles (middle) at $T = 450(30)$ nK (top, middle) and 390(30) nK (bottom) with no free parameters. Thickness represents temperature error [27,36].

identical fermions are suppressed: contributions from the s-wave incoming channel are forbidden while contributions from all higher-order partial waves become ever more kinematically suppressed. Indeed, no higher-order partial waves contribute well below the threshold of the p-wave centrifugal barrier ~50 μK [5,37]. Though differing in detail, for identical fermions, quantum statistics and kinematic suppression both play roles in the suppression of inelastic dipolar scattering and in the suppression of non-dipolar elastic scattering. In contrast, there is no p-wave threshold barrier in the bosonic case, since symmetrization allows an incoming s-wave channel.

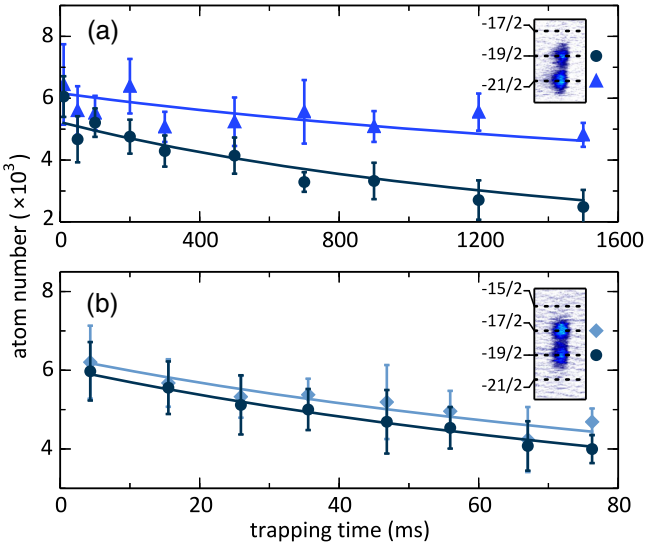

FIG. 4 (color online). Dipolar relaxation of spin mixtures. Curves are fits to coupled two-body-loss rate equations; see Ref. [27]. (a) Population decay of fermionic ^{161}Dy in the $m_F = -19/2$ (circles) and $m_F = -21/2$ (triangles) states at $T = 450(20)$ nK and $B = 0.410(5)$ G. (b) ^{161}Dy population decay in the $m_F = -17/2$ (diamonds) and $m_F = -19/2$ (circles) states at $T = 380(20)$ nK and 0.488(5) G. This inelastic collision proceeds more rapidly than panel (a)'s due to different quantum statistics; see text. Initial density of each spin state is $2(1) \times 10^{12}$ cm^{-3} [36]. (Insets) Averages of 18 Stern-Gerlach images.

We next investigate whether the fermionic suppression of dipolar relaxation is present in collisions involving spin mixtures. As predicted by theory, we observe suppression in the decay of the $m_F = -19/2, -21/2$ mixture, but no suppression in the decay of the $m_F = -17/2, -19/2$ mixture; see Fig. 4. These drastically different decay rates are due to the different quantum statistics governing the dominant relaxation processes. The only interspecies decay channel available to the $m_F = -19/2, -21/2$ mixture is $|-19/2; -21/2\rangle \rightarrow |-21/2; -21/2\rangle$, as depicted in Fig. 1(d). This process results in indistinguishable outgoing particles in the maximally stretched state $m_F = -F$ and, being the time-reversed process of that depicted in Fig. 1(a), exhibits fermionic suppression ($\epsilon = -1$).

In contrast, the decay of the $m_F = -17/2, -19/2$ mixture is dominated by the process $|-17/2; -19/2\rangle \rightarrow |-17/2; -21/2\rangle$ involving distinguishable mixtures in both the incoming and outgoing channels; see Fig. 1(f). This process exhibits no fermionic suppression because the particular particle flipping its spin is unambiguous since $\Delta m_f = \pm 2$ is not allowed for a single particle undergoing dipolar relaxation. This cross section is given by the $\epsilon = 0$ case of Eq. (2) with the different spin-dependent coefficient $F(F-2)^2\sigma_1/(2F^3)$ [27]. The measured and predicted interspecies β_{DR}'s are also listed in Table I. To measure

these rates, the spin populations are cotrapped and subsequently separated and imaged via a Stern-Gerlach measurement. The populations are fit to coupled rate equations, as shown in Fig. 4, see Ref. [27].

The enhancement in the dipolar relaxation of bosonic ^{162}Dy versus the magnetic field contrasts markedly with the suppression in fermionic ^{161}Dy. This manifestation of universal inelastic dipolar scattering demonstrates that dipolar relaxation is far less severe in highly dipolar fermions than in highly dipolar bosons and will be less of a hindrance to experiments using high-spin fermions in studies of quantum many-body physics. For example, observing ferronematicity or BCS superfluidity in Dy would require long-lived spin mixtures [18,20], as would experiments generating 1D spin-orbit coupling and non-Abelian gauge fields in 2D with Raman laser fields [23,38].

We acknowledge support from the AFOSR and NSF.

[1] C. Pethick and H. Smith, *Bose-Einstein Condensation in Dilute Gases* (Cambridge University Press, Cambridge, England, 2002).

[2] J. J. Sakurai and J. Napolitano, *Modern Quantum Mechanics* (Addison-Wesley, Reading, MA, 2011).

[3] K. Ni, S. Ospelkaus, D. Wang, G. Quemener, B. Neyenhuis, M. H. G. de Miranda, J. L. Bohn, J. Ye, and D. S. Jin, Nature (London) **464**, 1324 (2010).

[4] C. Cohen-Tannoudji and D. Guéry-Odelin, *Advances In Atomic Physics: An Overview* (World Scientific, Singapore, 2011).

[5] B. DeMarco, J. L. Bohn, J. P. Burke, M. Holland, and D. S. Jin, Phys. Rev. Lett. **82**, 4208 (1999).

[6] B. DeMarco and D. Jin, Science **285**, 1703 (1999).

[7] S. Hensler, J. Werner, A. Griesmaier, P. O. Schmidt, A. Görlitz, T. Pfau, S. Giovanazzi, and K. Rzażewski, Appl. Phys. B **77**, 765 (2003).

[8] J. L. Bohn, M. Cavagnero, and C. Ticknor, New J. Phys. **11**, 055039 (2009).

[9] B. Pasquiou, G. Bismut, Q. Beaufils, A. Crubellier, E. Maréchal, P. Pedri, L. Vernac, O. Gorceix, and B. Laburthe-Tolra, Phys. Rev. A **81**, 042716 (2010).

[10] Collisions between dipolar bosons include an additional pseudopotential contact term arising from the short-range van der Waals interaction in the s-wave channel.

[11] Here "universal" means short-range physics plays no role; scattering only depends on atomic parameters through μ and mass [8] and not on, e.g., the difficult-to-calculate phase shifts of partial waves at short range [12].

[12] C. Chin, R. Grimm, P. Julienne, and E. Tiesinga, Rev. Mod. Phys. **82**, 1225 (2010).

[13] M. Lu, N. Q. Burdick, and B. L. Lev, Phys. Rev. Lett. **108**, 215301 (2012).

[14] K. Aikawa, A. Frisch, M. Mark, S. Baier, R. Grimm, and F. Ferlaino, Phys. Rev. Lett. **112**, 010404 (2014).

[15] The moments of several highly dipolar species are [μ_{KRb}; μ_{Dy}; μ_{Er}; μ_{Cr}]=[0.57 Debye (saturated), 0.2D in Ref. [3]; 10 Bohr magnetons (μ_B); $7\mu_B$; $6\mu_B$].

[16] Though inelastic dipolar collisions can, in certain situations, lead to cooling [17].

[17] M. Fattori, T. Koch, S. Goetz, A. Griesmaier, S. Hensler, J. Stuhler, and T. Pfau, Nat. Phys. **2**, 765 (2006).

[18] I. Bloch, J. Dalibard, and W. Zwerger, Rev. Mod. Phys. **80**, 885 (2008).

[19] T. Lahaye, C. Menotti, L. Santos, M. Lewenstein, and T. Pfau, Rep. Prog. Phys. **72**, 126401 (2009).

[20] B. M. Fregoso and E. Fradkin, Phys. Rev. Lett. **103**, 205301 (2009).

[21] Y. Li and C. Wu, Sci. Rep. **2**, 392 (2012).

[22] B. Lian, T.-L. Ho, and H. Zhai, Phys. Rev. A **85**, 051606 (2012).

[23] X. Cui, B. Lian, T.-L. Ho, B. L. Lev, and H. Zhai, Phys. Rev. A **88**, 011601 (2013).

[24] M. A. Naides, R. W. Turner, R. A. Lai, J. M. DiSciacca, and B. L. Lev, Appl. Phys. Lett. **103**, 251112 (2013).

[25] B. K. Newman, N. Brahms, Y. S. Au, C. Johnson, C. B. Connolly, J. M. Doyle, D. Kleppner, and T. J. Greytak, Phys. Rev. A **83**, 012713 (2011).

[26] M. Lu, S.-H. Youn, and B. L. Lev, Phys. Rev. Lett. **104**, 063001 (2010).

[27] See Supplemental Material at http://link.aps.org/supplemental/10.1103/PhysRevLett.114.023201 for experimental details, data analysis, and cross section expressions, which includes Refs. [28,29].

[28] M. Lu, Ph.D. Thesis, Stanford, 2014.

[29] P. S. Julienne and F. H. Mies, J. Opt. Soc. Am. B **6**, 2257 (1989).

[30] Fermionic Dy possesses nuclear spin $I = 5/2$ and $F = J + I = 8 + 5/2 = 21/2$, where J is the total electronic angular momentum. Bosonic Dy is $I = 0$ ($F = J = 8$) and consequently lacks hyperfine structure [26,31,32].

[31] W. C. Martin, R. Zalubas, and L. Hagan, *Atomic Energy Levels–The Rare Earth Elements* (NSRDS-NBS, 60, Washington, D.C., 1978).

[32] M. Lu, S. H. Youn, and B. L. Lev, Phys. Rev. A **83**, 012510 (2011).

[33] The g factor is 1.242 for ^{162}Dy and 0.946 for ^{161}Dy [31].

[34] M. Lu, N. Q. Burdick, S. H. Youn, and B. L. Lev, Phys. Rev. Lett. **107**, 190401 (2011).

[35] K. Baumann, N. Q. Burdick, M. Lu, and B. L. Lev, Phys. Rev. A **89**, 020701(R) (2014).

[36] All errors represent one standard error.

[37] S. Kotochigova and A. Petrov, Phys. Chem. Chem. Phys. **13**, 19165 (2011).

[38] N. Goldman, G. Juzeliūnas, P. Ohberg, and I. B. Spielman, Rep. Prog. Phys. **77**, 126401 (2014).